High-level β-carotene production from xylose by engineered *Saccharomyces cerevisiae* without overexpression of a truncated *HMG1* (t*HMG1*)

Liang Sun[1,2], Christine Anne Atkinson[1,2], Ye-Gi Lee[1,2], Yong-Su Jin[1,2*]

[1]Department of Food Science and Human Nutrition, and [2]Carl R. Woese Institute for Genomic Biology, University of Illinois at Urbana-Champaign, Urbana, IL 61801

[*] Corresponding author: Yong-Su Jin

Tel: 217-333-7981, Fax: 217-333-0508, Email: ysjin@illinois.edu

Mailing address: 1206 W. Gregory Drive, Carl R. Woese Institute for Genomic Biology, Urbana, IL 61801, United States

ABSTRACT

β-carotene is a natural pigment and health-promoting metabolite, and has been widely used in the nutraceutical, feed and cosmetic industries. Here, we engineered a GRAS yeast *Saccharomyces cerevisiae* to produce β-carotene from xylose, the second most abundant and inedible sugar component of lignocellulose biomass. Specifically, a β-carotene biosynthetic pathway containing *crtYB*, *crtI* and *crtE* from *Xanthophyllomyces dendrorhous* was introduced into a xylose-fermenting *S. cerevisiae*. The resulting strain produced β-carotene from xylose at a titer three-fold higher than from glucose. Interestingly, overexpression of *tHMG1*, which has been reported as a critical genetic perturbation to enhance metabolic fluxes in the mevalonate (MVA) pathway and β-carotene production in yeast when glucose is used, did not further improve the production of β-carotene from xylose. Through fermentation profiling, metabolites analysis and transcriptional studies, we found the advantages of using xylose as a carbon source instead of glucose for β-carotene production to be a more respiratory feature of xylose consumption, a larger cytosolic acetyl-CoA pool, and up-regulated expression levels of rate-limiting genes in the β-carotene producing pathway, including *ACS1* and *HMG1*. As a result, 772.8 mg/L of β-carotene was obtained in a fed-batch bioreactor culture with xylose feeding. Considering the inevitable production of xylose at large scales when cellulosic biomass-based bioeconomy is implemented, our results suggest xylose utilization is a promising strategy for overproduction of carotenoids and other isoprenoids in engineered *S. cerevisiae*.

KEYWORDS: β-carotene; xylose; glucose; t*HMG1*; *Saccharomyces cerevisiae*

INTRODUCTION

Carotenoids are a diverse class of C_{40} isoprenoids widely produced by plants, bacteria, fungi and microalgae (Berman et al., 2015; Henríquez, Escobar, Galarza, & Gimpel, 2016).

Of all known carotenoids, β-carotene is believed to be the most important due to its nutritional role as pro-vitamin A (Dowling & Wald, 1960) and health-promoting potential as an antioxidant (Palozza & Krinsky, 1992) and an anti-tumor agent (Williams, Boileau, Zhou, Clinton, & Erdman, 2000). Its wide applications in nutraceutical, feed and cosmetic industries lead to a fast-growing world market (Irwandi Jaswir, 2011). Currently, chemical synthesis remains the major route of commercial β-carotene production. Considering the safety concerns of chemical synthesis, and consumer preferences for natural additives, microbial production of β-carotene via metabolic engineering gains increasing interests and becomes an attractive alternative (Yoon et al., 2007; Zhao et al., 2013). The biological pathway of all isoprenoids use isopentenyl diphosphate (IPP) as precursor, which is synthesized through either MVA pathway in eukaryotes, or the 2-C-methyl-D-erythritol-4-phosphate (MEP) pathway in prokaryotes. Among potential microbial hosts, *Saccharomyces cerevisiae* has superior traits in industrial production of isoprenoids such as the GRAS (generally recognized as safe) status, ease of genetic manipulation, industrial robustness (Auesukaree et al., 2009), and the native MVA pathway which is generally considered as an effective supplier of isoprenoid precursor from acetyl-CoA (Vickers, Williams, Peng, & Cherry, 2017).

Researchers expend great efforts in heterologous production of carotenoids using engineered *S. cerevisiae*. Those efforts have far involved the optimization of metabolic flux, and balancing necessary cofactors by manipulating the expression levels of targeted genes (Das et al., 2007; Peralta-Yahya et al., 2011; Verwaal et al., 2007; Yan, Wen, & Duan, 2012). Among all the reported manipulation targets, overexpression of a truncated, soluble form of 3-hydroxy-3-methylglutaryl-coenzyme A reductase (t*HMG1*), a major rate-limiting enzyme of the MVA pathway, has been consistently recognized as an essential strategy for high-level production of carotenoids (Verwaal et al., 2007; Xie, Lv, Ye, Zhou, & Yu, 2015; Zhou et al., 2017) and other isoprenoids, such as artemisinic acid (Ro et al., 2006), farnesene (Meadows

et al., 2016), squalene and amorphadiene (Kwak et al., 2017) in *S. cerevisiae*. In addition to t*HMG1* overexpression, up-regulation of the MVA pathway related genes such as *ERG8*, *ERG12*, *ERG19*, *IDI1*, *ERG20* (Y. Sun, Sun, Shang, & Yan, 2016) and down-regulation of the ergosterol pathway related genes such as *ERG9* (Yan et al., 2012) have been attempted to increase the production of carotenoids.

Despite intensive genetic perturbations for driving metabolic fluxes towards carotenoids production, ethanol remains a major product due to the entirely fermentative metabolism of *S. cerevisiae* on glucose even in the presence of oxygen (Pfeiffer & Morley, 2014), which hindered the high-level production of carotenoids. This well-known metabolic regulation, termed the Crabtree effect, was not observed while using non-native sugar xylose as a carbon source (Y.-S. Jin, Laplaza, & Jeffries, 2004; Kwak et al., 2017; Matsushika, Goshima, & Hoshino, 2014). We, therefore, assumed that xylose fermentation by engineered *S. cerevisiae* might facilitate carotenoids production by alleviating glucose-dependent repression on respiratory metabolism. Additionally, xylose, comprising up to 30-40 % of lignocellulosic biomass, is the second most abundant sugar in nature that derived from non-edible sources (Kim, Ha, Wei, Oh, & Jin, 2012). Efficient production of value-added chemicals like carotenoids and other isoprenoids from xylose is an important step toward economical and sustainable bioconversion processes of lignocellulosic biomass (Kwak, Jo, Yun, Jin, & Seo, 2019). However, there was no attempt to synthesize carotenoids from xylose in engineered *S. cerevisiae* prior to our studies. As such, we constructed an engineered *S. cerevisiae* strain SR8B capable of producing β-carotene from xylose by introducing a β-carotene biosynthetic pathway containing *crtYB*, *crtI* and *crtE* from *X. dendrorhous* into a xylose-fermenting strain SR8. The strain SR8B was also used to convert the xylose-enriched hydrolysates from bioenergy sorghum into β-carotene (Cheng, Sun, Jin, Dien, & Singh, 2020). In another study, we enabled vitamin A production by integrating a β-carotene 15,15'-

monooxygenase into the SR8B strain and improved the production of vitamin A by xylose utilization and two-phase *in situ* extraction (L. Sun et al., 2019).

In this study, we observed increased production of β-carotene from xylose as compared to glucose in engineered *S. cerevisiae* SR8B. In order to explore the advantageous traits of xylose utilization for β-carotene production in engineered yeast, we assessed the differences in β-carotene production patterns from glucose and xylose via fermentation profiling, metabolites analysis and comparative transcriptional studies. High-level production of β-carotene was achieved using xylose as a carbon source without t*HMG1* overexpression and other genetic perturbations. This study demonstrated that using xylose as a carbon source would be a promising strategy for high-level and sustainable production of carotenoids and other isoprenoids in *S. cerevisiae*.

MATERIALS AND METHODS

Strain Construction. The strains, plasmids and PCR primers used in this study are listed in Table 1 and Table S1, respectively. Standard molecular biology procedures were conducted as described previously (Green, Sambrook, & Sambrook, 2012). The integration plasmid YIplac211YB/I/E* (Verwaal et al., 2007) was used to construct the SR8B strain. The detailed integration method was described in the **Supplementary Information**. A CRISPR/Cas9 system was applied for overexpression of catalytic domain of *HMG1* (*tHMG1*) by genomic integration. The Cas9-NAT plasmid (Addgene#64329) was transformed into the SR8B strain before Cas9-based genetic modifications. The t*HMG1* gene flanked by a strong constitutive yeast promoter *TDH3* and terminator *CYC1* was amplified from the plasmid pRS425TDH-tHMG1 as a donor DNA. The plasmid pRS42H-CS5 coding for guide RNA which targets the

intergenic site on Chr XV was co-transformed with the donor DNA fragments. Cells were selected on YPD plate supplemented with 120 μg/mL nourseothricin and 300 μg /mL Hygromycin B. Positive colonies were confirmed by diagnostic PCR and designated as the SR8BH strain.

Yeast Culture for the Production of β-carotene. To compare β-carotene production on glucose and xylose by engineered yeast, the engineered strains were inoculated from glycerol stocks into 5mL of a modified Verduyn medium (van Hoek, de Hulster, van Dijken, & Pronk, 2000) containing 20 g/L glucose or xylose as pre-cultures for glucose and xylose main cultures, respectively. The composition of the modified Verduyn medium was described previously (L. Sun et al., 2019). After pre-cultures for 2-3 days, cells were harvested and re-inoculated at an initial optical cell density of 1 at 600nm (OD_{600}) into main culture flasks, which were 250 mL baffled flasks with 50 mL of Verduyn medium containing either 40g/L glucose, or 40g/L xylose. Culture media were buffered with potassium hydrogen phthalate at a working concentration of 50 mM and pH of 5.5. We conducted aerobic batch fermentation experiments in a shaking incubator at 30 ℃ and 300 rpm. For a xylose fed-batch fermentation, the engineered strain was pre-cultured for 48 hours in 200 mL of Verduyn medium containing 40 g/L xylose at 30 ℃ and 300 rpm. The fed-batch fermentation was conducted in a 3-liter fermenter (New Brunswick Scientific-Eppendorf, Enfield, CT) with 1 L of Verduyn medium at 30 ℃. Initial xylose concentration was 87.1 g/L and additional amounts of xylose were fed to reach 40 ± 5 g/L of xylose upon depletion. The pH was maintained at 5.5 by automatically pumping in 4M NaOH. The gas flow rate was kept at 2 vvm, and agitation rate varied in the range of 500-800 rpm.

Quantitative Analysis. We monitored a cell density of each culture by measuring OD_{600} using a spectrophotometer (BioMate 5; Thermo Fisher Scientific, Waltham, USA). The dry cell weight (DCW) was then calculated from the measured OD_{600} by multiplying a conversion factor of 0.41 (1 OD_{600} =0.41 g DCW/L). To calibrate the conversion factor between optical density and dry cell weight, yeast cells were grown in the Verduyn medium, harvested by centrifugation at 10,000 rpm, and washed two times with distilled water. Washed cell pellets were resuspended in distilled water to various optical densities and filtrated via dried cellulose acetate membrane filters. After cell filtration, membrane filters were dried to constant weight in an 80°C convection oven and then weighed. Glucose, xylose, xylitol, glycerol, acetate and ethanol in the culture broth were quantified using high-performance liquid chromatography (HPLC, Agilent 1200 Series, Agilent Technologies, Wilmington, US) equipped with a refractive index detector and the Rezex ROA-Organic Acid H+ (8%) column (Phenomenex Inc, Torrance, CA). The diluted culture supernatants were analyzed at 50 ℃ with 0.005 M H_2SO_4 as the mobile phase. The flow rate was set at 0.6 mL/min.

β-carotene was extracted using acetone and quantified by measuring the absorbance at 453 nm (OD_{453}) with spectrophotometer as described previously (Yuan, Rouvière, LaRossa, & Suh, 2006). Specifically, cells were harvested from 1 mL culture broth by centrifugation. The cell pellets were resuspended with 1 mL acetone in a 2 mL screwed cap tube and crushed by a BeadBeater (BioSpec, USA). Samples were then centrifuged, and colored supernatants were collected in a 5 mL tube for measuring OD_{453}. The extraction procedure was repeated for three times until the cell pellets turned white. A standard curve (**Fig. S1**) was obtained by measuring OD_{453} of a serial of β-carotene standard (Cat. No. C4582, Sigma, USA) solution with known concentration using spectrophotometer. The standard curve was then used to

161 calculate the volumetric titer and specific content of β-carotene produced by engineered
162 strains.

163 For analysis of ergosterol production, 2 mL of fermentation broth was centrifuged to
164 separate the cells. The cell pellets were resuspended with 0.6 mL of extraction solution (50%
165 KOH: C_2H_5OH = 2: 3), and the mixture was saponified by incubating in 85 °C water bath for
166 2 hours. After chilling on ice, the saponified mixture was thoroughly mixed with 0.6 mL n-
167 heptane to extract the sterol. After centrifugation, a total 0.5 mL of n-heptane layer was
168 collected and dried in a centrifugal vacuum concentrator. Dried samples were dissolved in 0.5
169 mL of acetonitrile and analyzed using Shimadzu HPLC system equipped with a UV detector
170 (Shimadzu SPD-20A) and a C18 column (Phenomenex Kinetex 5 μL C18). Ergosterol was
171 separated with 100% acetonitrile at a flow rate of 2 mL/min and detected by UV absorbance
172 at 280 nm. A standard curve (**Fig. S2**) was prepared using authentic ergosterol standard (Cat.
173 No. 45480, Sigma, USA) for calculating ergosterol concentration from each sample.

174 Lipid weight was determined as previously described (Zhang et al., 2016). Briefly, 2
175 mL cell cultures with OD_{600} adjusted at 10 were centrifuged at 15,000 rpm for 1 min. Cell
176 pellets were transferred into 15-mL glass centrifuge tubes and were crushed using
177 BeadBeater with 6 mL of chloroform/methanol (1:1 volumetric). The samples were then
178 mixed with 1.5 mL water and vortexed for 1 min. After centrifugation, the organic layer was
179 collected, washed with 1.5 mL of 0.1% (w/v) NaCl water solution, and dried overnight at
180 room temperature in a preweighed tube. The tube was further dried in an oven at 80 °C until
181 they reached a constant weight to determine lipid content. Total lipid content was calculated
182 from the final tube weight by subtraction of original tube weight and the corresponding β-
183 carotene content for each sample.
184

Identification of Carotenoids Composition. To identify the carotenoids composition by HPLC, yeast extracts from glucose and xylose batch fermentation were separated on a reverse-phase C30 HPLC column (4.6 × 150 mm, 3 μm; YMC, Wilmington, NC) maintained at 18°C, and detected by a photodiode array detector (model 2996; Waters, Milford, MA) as previously described (Yeum et al., 1996). β-carotene, phytoene (Cat. No. 78903, Sigma, USA) and lycopene (Cat. No. SMB00706, Sigma, USA) standards were used for the identification.

Visualization of Lipid Bodies. Lipid bodies were visualized using confocal microscope after staining as described previously (Beopoulos et al., 2008). Fresh cells were harvested at exponential phase from a batch fermentation with either glucose (19 hour) or xylose (31 hour) as carbon source (**Fig. S3**) and resuspended at OD_{600} 20. Nile red (Cat. No. 72485, Sigma, USA) solution in acetone (1 mg/ml) was added to the cell suspensions (1/10 vol/vol). The mixtures were incubated at room temperature for 1 hour to stain and identify lipids. After washing with saline, cells were resuspended to OD_{600} 20 in 50 mM potassium hydrogen phthalate buffer and immobilized using low melting-point agarose (Fisher Scientific, Hampton, NH) on a Fluorodish™ (World Precision Instruments, USA) for viewing. Stained cells were viewed and photographed with a confocal microscope (Zeiss LSM 700, Carl Zeiss AG, Oberkochen, Germany) using an oil immersion objective (63×) at 633 nm radiation.

Real-time qPCR Quantification of mRNA. We conducted real-time qPCR analysis to investigate the expression levels of related genes. Total RNA was extracted and purified using MasterPure™ Yeast RNA Purification Kit (Epicentre, USA) following the attached protocol. RNA was reverse transcribed to cDNA using a cDNA synthesis kit (iScript™, Bio-Rad, Canada). Real-time qPCR was performed in a LightCycler® 480 Real Time PCR

system (Roche, Swiss) using SsoAdvanced™ Universal SYBR® Green Supermix (Bio-Rad, Canada) and qPCR amplicon primers (**Table S2**). The housekeeping gene *ACT1* was used as the control. Relative gene expression of xylose condition *versus* glucose condition was calculated using the $2^{-\Delta\Delta Ct}$ method and presented as fold change (Livak & Schmittgen, 2001).

RESULTS

Construction of a Xylose-fermenting, β-carotene-producing *S. cerevisiae*. We engineered the GRAS yeast *S. cerevisiae* to functionally express the heterologous β-carotene synthetic pathway and produce β-carotene from xylose as well as glucose (**Fig. 1**, **Fig. 2**). Specifically, *crtE*, *crtI*, *crtYB* genes from *X. dendrorhous* coding for GGPP synthase, phytoene desaturase, phytoene synthase and lycopene cyclase, respectively, in the β-carotene biosynthesis pathway were integrated into the genome of the *S. cerevisiae* SR8, previously engineered to ferment xylose (Kim et al., 2013). The resulted strain was named as the SR8B strain.

Comparison of β-carotene Production Patterns on Glucose and Xylose. When xylose was used as a carbon source, we observed the SR8B cell cultures always exhibited an intense orange color while those using glucose appeared as light yellow (**Fig. 1B**). We suspected that carotenoids other than β-carotene might be produced and the composition of carotenoids in the cells grown on glucose and xylose might be different. To identify the carotenoids composition produced by engineered yeast cells grown on different carbon sources, cells cultured either on glucose or on xylose were harvested for carotenoids extraction and HPLC analysis. β-carotene was the predominant carotenoid produced on both conditions according to the chromatographs (**Fig. 2**), while the β-carotene peak in the chromatograph of xylose

culture showed much higher intensity than that of glucose culture (**Fig. 2**). The intermediates phytoene and lycopene also accumulated in xylose cultures, while only phytoene was detected in glucose condition with a lower peak intensity (**Fig. 2**).

The engineered SR8B strain was cultured aerobically on glucose and xylose to compare differences in fermentation profiles and β-carotene production patterns. When cultured on glucose, the engineered strain fermented glucose into a large amount of ethanol, and then started to reassimilate ethanol as carbon source (**Fig. 3A**). In contrast, when cultured on xylose, the strain consumed xylose slower with negligible amounts of ethanol production but showed a higher cell mass titer and more glycerol accumulation (**Fig. 3B**). In terms of β-carotene production, a rapid fermentation of glucose, and subsequent ethanol consumption led to much less production of β-carotene as compared to xylose culture where xylose was consumed steadily with little ethanol production (**Fig. 3C**, **Fig.3D**). As a result, the SR8B strain accumulated β-carotene intracellularly with a specific content of 13.7 mg/g DCW and a volumetric titer of 96.4 mg/L from 40 g/L xylose. These are approximately two-fold and three-fold higher than 3.9 mg/g DCW and 24.2 mg/L of β-carotene produced from 42 g/L glucose (**Fig. 3C**, **Fig. 3D**).

Effect of t*HMG1* Overexpression on β-carotene Production using Xylose as a Carbon Source. To further enhance β-carotene production by engineered strain from xylose, HMG-CoA reductase, a well-known rate-controlling enzyme in the MVA pathway, was selected as the manipulation target (**Fig. 1A**). Specifically, an expression cassette containing a truncated *HMG1* (t*HMG1*) coding for the catalytic domain of HMG-CoA reductase under the control of *TDH3* promoter was integrated into the genome of the SR8B strain using Cas9-based genome editing. The resulting t*HMG1* overexpressing strain, named as the SR8BH strain, showed lower cell mass titers as compared to the SR8B strain on both glucose and xylose condition

(**Fig. S4**). As expected, the SR8BH strain accumulated more β-carotene (6.5 mg β-carotene/g DCW) than the SR8B strain (3.9 mg β-carotene/g DCW) when glucose was used as a carbon source (**Fig. 4**). While, interestingly, under xylose fermentation, no improvement on β-carotene production was observed in the SR8BH strain (12.0 mg β-carotene/g DCW) compared to the SR8B strain (13.7 mg β-carotene/g DCW) (**Fig. 4**).

Effect of Xylose Utilization on the Production of Ergosterol and Lipids. In order to examine broader impacts of using xylose as a carbon source on other cytosolic acetyl-CoA derived products, cells were taken at the end of fermentation of the SR8B strain for ergosterol and lipid analysis. The SR8B strain accumulated ergosterol with a specific content of 17.0 ± 0.6 mg/g DCW from xylose which was 28% more than using glucose, and a higher improvement of 69% in volumetric titer was observed due to the improved cell mass titer in xylose fermentation (**Fig 5A**).

To investigate the effect of xylose utilization on lipids production by the SR8 strain, cells harvested from glucose and xylose cultures were stained and visualized under a confocal microscope. The cells grown on xylose were found to accumulate more lipid bodies (LB) with larger size than cells grown on glucose, leading to a bigger portion of the stained LB to the cell area (**Fig. 5B**). The enhanced LB formation suggested a greater lipids production capacity of engineered yeast on xylose fermentation, and this was confirmed by the lipids weight analysis. The engineered SR8B strain produced lipids through xylose utilization with a specific content 58% higher than glucose utilization (43.1 vs. 27.2 mg lipids/g DCW) (**Fig. S5**).

Comparison of Transcription Profiles of the Genes involved in β-carotene Biosynthesis in Engineered Yeast on Glucose and Xylose. To further reveal the potential mechanisms of

improved production by xylose utilization, transcriptional analysis was carried out on genes related to cytosolic PDH bypass (*ACS1* and *ACS2*), lipid biosynthesis pathway (*ACC1*), MVA pathway (*ERG10*, *ERG13*, *HMG1*, *HMG2*, *ERG12*, *ERG8*, *ERG19*, *IDI1*, and *ERG20*) and ergosterol pathway (*ERG9*) (**Fig. 1C**). Cells for mRNA extraction and quantification were taken at the exponential phase of glucose and xylose fermentation by the SR8B strain, which is 19 hours and 31 hours, respectively (**Fig. S3**). While most of the 13 genes studied did not show significant difference in transcriptional levels between glucose and xylose culture conditions, the expression levels of gene *ACS1* coding for acetyl-CoA synthase and gene *HMG1* coding for HMG-CoA reductase increased significantly in response to xylose substitution, where 2.7 ± 0.1 and 2.2 ± 0.2-fold differences were observed, respectively.

Xylose Fed-batch Fermentation for the Production of β-carotene. The capacity of β-carotene production from xylose by the engineered strain SR8B was assessed in a 3-liter bioreactor via a fed-batch fermentation. Cells were inoculated at an initial cell density of OD_{600} = 3.1, and cultured with 87 g/L of xylose (**Fig. 6**). Upon the depletion of initially added xylose, additional xylose was provided to reach a concentration of 40 ± 5 g/L of xylose. The feeding was repeated seven times until the β-carotene titer was saturated. Despite the presence of high concentrations of xylose in the medium, ethanol accumulation was negligible during the fed-batch culture. Finally, cell density reached to OD_{600} of 165.9 (68.0 g DCW/L) and 772.8 mg/L of β-carotene was produced with a productivity of 5.4 mg/L/h (**Fig. 6**). The final β-carotene yield was 2.2 mg β-carotene/g xylose and specific content was 11.4 mg β-carotene/g DCW. In addition, a large amount of glycerol (30.1 g/L) and acetate (22.5 g/L) were accumulated at the end of fermentation.

DISCUSSION

Over the past 20 years, researchers have made great efforts in enabling efficient ethanol production from anaerobic fermentation of xylose, the second most abundant and inedible sugar component of lignocellulose biomass, in engineered yeast as an important step towards a robust second-generation biofuels industry (Yong-Su Jin, Lee, Choi, Ryu, & Seo, 2000; Kim et al., 2013). Recently, production of high-value metabolites, such as astaxanthin (Montanti, Nghiem, & Johnston, 2011), protopanaxadiol (Gao, Caiyin, Zhao, Wu, & Lu, 2018), squalene, and amorphadiene (Kwak et al., 2017), from aerobic xylose fermentation by engineered yeast has gained increasing interest due to the respiratory traits of xylose metabolism and the attracting economic profitability of biomass conversion (Kwak et al., 2019).

For the first time, we engineered a yeast *S. cerevisiae* to produce β-carotene from xylose. As compared to the conventional sugar glucose, xylose exhibited superior traits as a carbon source for the production of β-carotene in engineered *S. cerevisiae*. When cultured on xylose under aerobic conditions, the engineered strain SR8B produced remarkably less ethanol as compared when glucose was used as a carbon source (**Fig. 3**). This is attributed to the dysregulation effect of xylose on the glucose-dependent repression of the respiratory metabolism (Y.-S. Jin et al., 2004; Matsushika et al., 2014). As such, the engineered yeast produced β-carotene at a much higher yield from xylose (2.4 mg β-carotene /g xylose) than from glucose (0.4 mg β-carotene/ g glucose). As the xylose consumption was slower than glucose, the glucose cultures were extended to the ethanol consumption phase for a fair comparison. Nevertheless, the net production of β-carotene from sequential utilization of glucose and ethanol was still much lower than that from xylose culture regarding both volumetric titer and specific content (**Fig. 3**). In addition, a lower cell density was observed on glucose condition as compared to a corresponding xylose condition. This might be associated with the energetically high-cost conversion of ethanol into cytosolic acetyl-CoA in

S. cerevisiae which restricts the yield of biomass or products that require ATP (Kok et al., 2012). The higher yield of cell biomass from xylose is another contributory factor of the enhanced β-carotene titer as cell concentration is important for the volumetric titers of intracellular metabolites.

Overexpression of t*HMG1* was critical to high-level production of β-carotene and other isoprenoids by engineered yeast, as described in previous reports (Verwaal et al., 2007; Xie et al., 2014). As such, we overexpressed t*HMG1* in the SR8B strain to further increase β-carotene production on xylose cultures. As expected, the newly constructed strain SR8BH produced β-carotene with a higher specific content than the SR8B strain while cultured on glucose (**Fig. 4**). However, t*HMG1* overexpression did not result in any improvement of β-carotene production from xylose (**Fig. 4**). More interestingly, the beneficial effects of using xylose instead of glucose as a carbon source on β-carotene production (a 254% improvement in β-carotene specific content by SR8B strain) appeared to be much stronger than that of t*HMG1* overexpression on glucose condition (a 67% improvement in β-carotene specific content by SR8BH strain as compared to SR8B strain). These results suggested that using xylose as a carbon source in substitution for glucose is an effective strategy to increase β-carotene production in *S. cerevisiae* without t*HMG1* overexpression and other genetic manipulations.

The higher production of β-carotene and accumulation of intermediates (phytoene and lycopene) (**Fig. 2**, **Fig. 3**) suggested a better supply of precursors for the carotenogenic pathway when xylose was used as a carbon source as compared to glucose (Verwaal et al., 2007). To investigate the effects of xylose utilization on metabolic flux related to β-carotene biosynthesis, the accumulation of endogenous ergosterol and lipids was monitored as their biosynthesis competes with the carotenogenic pathway for common precursors farnesyl pyrophosphate (FPP) and cytosolic acetyl-CoA, respectively (**Fig. 1A**). We observed that the

engineered strain produced more ergosterol on xylose cultures as compared to glucose cultures (**Fig. 5A**). This might be attributed to a stronger metabolic flux through the MVA pathway that provides sufficient supply of FPP. Alternatively, the use of xylose as a carbon source under aerobic conditions might have stimulated the transcription of genes in sterol biosynthesis pathway. In addition to the improved ergosterol accumulation, cells grown on xylose were found to accumulate more lipids as compared to those grown on glucose (**Fig. 5B**, **Fig. S5**), which could possibly be interpreted as a result of increased cytosolic acetyl-CoA availability. Moreover, the increased lipids content might have promoted the accumulation of β-carotene as well as ergosterol by expanding cell-storage capacity for lipophilic end products (Kwak et al., 2019; Ma et al., 2019; Sorger, Athenstaedt, Hrastnik, & Daum, 2004). These results would also provide clues to sterols and lipids biosynthesis from cellulosic biomass.

Previous reports demonstrated that xylose utilization in engineered *S. cerevisiae* leads to distinct transcriptional patterns of genes involved in various metabolic pathways as compared to glucose utilization (Y.-S. Jin et al., 2004; Kwak et al., 2017; Matsushika et al., 2014). Thus, we investigated the effect of xylose on expression levels of genes related to cytosolic PDH bypass, lipid synthesis, MVA pathway and ergosterol pathway via comparative real-time qPCR. Among all the genes studied, *ACS1* and *HMG1* were highly expressed when the cells were grown on xylose as compared to glucose, while others did not show significant difference in expression levels (**Fig. 1C**). It is known that the transcription of *ACS1* gene coding for acetyl-CoA synthase is subject to glucose repression (Berg et al., 1996). Therefore, we reason that using xylose instead of glucose as carbon source leads to the alleviation of the glucose-dependent repression on the transcription of *ACS1*, thus resulting in greater abundance of cytosolic acetyl-CoA as building blocks for lipids, ergosterol and β-carotene synthesis. As a key rate-limiting gene in the MVA pathway, *HMG1* was an essential

target for manipulation in order to overproduce terpenes and sterols in *S. cerevisiae*. Overexpression of native or heterologous *HMG1* in engineered *S. cerevisiae* was shown to be beneficial for β-carotene production in previous studies (Li, Sun, Li, & Zhang, 2013; Yan et al., 2012). Accordingly, the improved transcriptional level of *HMG1* by xylose utilization could have further promoted the conversion of the abundant cytosolic acetyl-CoA into FPP as a precursor for β-carotene and ergosterol. This might be the reason why t*HMG1* overexpression was neither necessary nor desirable for β-carotene overproduction while xylose was used as a carbon source.

Owing to the peculiar physiologic characteristics of xylose fermentation, including low ethanol production and high cell mass yield, a high cell density culture of the SR8B strain was achieved through intermittent xylose feeding instead of further genetic perturbations, or sophisticated feeding algorithms. Consequently, a final β-carotene titer of 772.8 mg/L was obtained (**Fig. 6**). This titer is even slightly higher than the best β-carotene titer (750 mg/L) previously reported in engineered *S. cerevisiae* (López et al., 2019). In the previous study, the researchers examined the highest-carotenoid-accumulating yeast strain SM14 obtained from adaptive evolution experiments (Reyes, Gomez, & Kao, 2014) in optimized glucose fed-batch cultures. However, the β-carotene productivity (5.0 mg/L/h) in our study is substantially lower than that of the previous study (10.9 mg/L/h), suggesting a large room for improvement. Besides, the final yield (2.2 mg β-carotene/g xylose) and specific content (11.4 mg β-carotene/g DCW) of β-carotene was relatively lower than those of the batch fermentation (2.4 mg β-carotene/g xylose & 13.7 mg β-carotene/g DCW, respectively). This might be attributed to the large amount of glycerol and acetate accumulation which consumed noticeable carbon sources and energy. The considerable accumulation of glycerol and acetate indicates that the engineered yeast cells might suffer from NADH/NAD^+ redox and energy imbalance. Our previous studies also reported

substantial accumulation of glycerol in xylose fed-batch fermentations (Kwak et al., 2017; L. Sun et al., 2019). The redox imbalance in xylose metabolism was known to be caused by the different cofactor dependences of XR (xylose reductase) and XDH (xylitol dehydrogenase) in xylose assimilation pathway (Kwak et al., 2019). Accordingly, strategies to eliminate the glycerol and acetate accumulation, such as using a NADH-preferred *Spathaspora passalidarum* Xyl1.2 in xylose assimilation pathway (Hou, 2012), replacing native NADPH-specific *HMG1* into a NADH-specific *Silicibacter pomeroyi HMG1* in the MVA pathway (Meadows et al., 2016), or rising the aeration by increasing the rate of agitation and supply of air, could lead to a further enhanced capacity of β-carotene production from xylose by our engineered yeast. Despite the highest titer by our engineered strain, the relatively low productivity and yield might hamper economically feasible implementation of β-carotene production from pure xylose. As such, we have been seeking to produce β-carotene from xylose-enriched cellulosic hydrolysates (Cheng et al., 2020). In addition to the above-mentioned optimizations, our efforts could lead to a sustainable and environmental-friendly alternative to the current chemical synthesis routes for β-carotene production.

In conclusion, we constructed an engineered *S. cerevisiae* strain capable of producing β-carotene from xylose—the second most abundant and non-edible sugar in nature. As compared to the conventional sugar glucose, xylose displayed superior traits as a carbon source for the production of β-carotene in engineered *S. cerevisiae*, including a lower ethanol production, a higher cell mass yield, a larger cytosolic acetyl-CoA pool and up-regulated expression levels of rate-limiting genes. Hence, high-level β-carotene production in engineered *S. cerevisiae* was achieved in a fed-batch bioreactor simply through xylose feeding instead of intensive genetic perturbations or culture optimization. Our findings suggest xylose utilization is a promising strategy for overproduction of carotenoids and other isoprenoids in engineered *S. cerevisiae*.

ACKNOWLEDGEMENT

This work was funded by the DOE Center for Advanced Bioenergy and Bioproducts Innovation (U.S. Department of Energy, Office of Science, Office of Biological and Environmental Research under Award Number DE-SC0018420). Any opinions, findings, and conclusions or recommendations expressed in this publication are those of the author(s) and do not necessarily reflect the views of the U.S. Department of Energy. The authors would like to thank Dr. Rene Verwaal in Nertherland and Dr. Guo-liang Yan in China for kindly providing the plasmid YIplac211YB/I/E*. The authors also thank Dr. John W. Erdman and Molly Black in the University of Illinois for their earnest help with the carotenoids chromatography.

ASSOCIATED CONTENT

Supporting Information

Table S1. Primers for strain construction. Table S2. Primers for qPCR amplicons. Fig. S1. Standard curve for calculating β-carotene concentration. Fig. S2. Standard curve for calculating ergosterol concentration. Fig. S3. Growth curves of SR8B strain on glucose and xylose (lnX vs. t). Fig. S4. Batch fermentation profiles of engineered *S. cerevisiae* SR8BH on glucose and xylose. Fig. S5. Lipids production by engineered SR8B strain through glucose and xylose utilization.

AUTHOR INFORMATION

Corresponding Author

*E-mail: ysjin@illinois.edu.

Present Addresses: 1206 West Gregory Drive, Urbana, IL 61801

ORCID:

Yong-Su Jin: 0000-0002-4464-9536

Liang Sun: 0000-0001-8826-7276

Christine Anne Atkinson: 0000-0002-8790-6782

Ye-Gi Lee: 0000-0002-7473-1493

Author Contributions

Y.-S.J., L.S. developed the idea of this work. Y.-S.J., L.S. designed the experiments. L.S. performed the experiments. L.S., C.A., Y.-G.L. and Y.-S.J. wrote the manuscript.

Funding

This work was funded by the DOE Center for Advanced Bioenergy and Bioproducts Innovation (U.S. Department of Energy, Office of Science, Office of Biological and Environmental Research under Award Number DE-SC0018420). Any opinions, findings, and conclusions or recommendations expressed in this publication are those of the author(s) and do not necessarily reflect the views of the U.S. Department of Energy. L. S. would like to thank the China Scholarship Council (CSC) for financial support.

Notes

The authors declare no competing financial interest.

ABBREVIATIONS USED

tHMGR, truncated 3-hydroxy-3-methylglutaryl-coenzyme A reductase gene; IPP, isopentenyl diphosphate; FPP, farnesyl pyrophosphate; GGPP, geranylgeranyl pyrophosphate; MVA,

mevalonate; MEP, 2-C-methyl-D-erythritol-4-phosphate; GRAS, generally recognized as safe; DCW, dry cell weight; LB, lipid body

REFERENCES

Auesukaree, C., Damnernsawad, A., Kruatrachue, M., Pokethitiyook, P., Boonchird, C., Kaneko, Y., & Harashima, S. (2009). Genome-wide identification of genes involved in tolerance to various environmental stresses in *Saccharomyces cerevisiae*. *Journal of Applied Genetics*, *50*(3), 301–310. doi: 10.1007/BF03195688

Beopoulos, A., Mrozova, Z., Thevenieau, F., Dall, M.-T. L., Hapala, I., Papanikolaou, S., … Nicaud, J.-M. (2008). Control of Lipid Accumulation in the Yeast *Yarrowia lipolytica*. *Applied and Environmental Microbiology*, *74*(24), 7779–7789. doi: 10.1128/AEM.01412-08

Berg, M. A. van den, Jong-Gubbels, P. de, Kortland, C. J., Dijken, J. P. van, Pronk, J. T., & Steensma, H. Y. (1996). The Two Acetyl-coenzyme A Synthetases of *Saccharomyces cerevisiae* Differ with Respect to Kinetic Properties and Transcriptional Regulation. *Journal of Biological Chemistry*, *271*(46), 28953–28959. doi: 10.1074/jbc.271.46.28953

Berman, J., Zorrilla-López, U., Farré, G., Zhu, C., Sandmann, G., Twyman, R. M., … Christou, P. (2015). Nutritionally important carotenoids as consumer products. *Phytochemistry Reviews*, *14*(5), 727–743. doi: 10.1007/s11101-014-9373-1

Cheng, M.-H., Sun, L., Jin, Y.-S., Dien, B., & Singh, V. (2020). Production of xylose enriched hydrolysate from bioenergy sorghum and its conversion to β-carotene using an engineered *Saccharomyces cerevisiae*. *Bioresource Technology*, *308*, 123275. doi: 10.1016/j.biortech.2020.123275

Das, A., Yoon, S.-H., Lee, S.-H., Kim, J.-Y., Oh, D.-K., & Kim, S.-W. (2007). An update on microbial carotenoid production: Application of recent metabolic engineering tools. *Applied Microbiology and Biotechnology*, *77*(3), 505. doi: 10.1007/s00253-007-1206-3

Dowling, J. E., & Wald, G. (1960). The Biological Function of Vitamin A Acid. *Proceedings of the National Academy of Sciences of the United States of America*, *46*(5), 587–608.

Gao, X., Caiyin, Q., Zhao, F., Wu, Y., & Lu, W. (2018). Engineering *Saccharomyces cerevisiae* for Enhanced Production of Protopanaxadiol with Cofermentation of Glucose and Xylose. *Journal of Agricultural and Food Chemistry*, *66*(45), 12009–12016. doi: 10.1021/acs.jafc.8b04916

Green, M. R., Sambrook, J., & Sambrook, J. (2012). *Molecular cloning: A laboratory manual* (4th ed). Cold Spring Harbor, N.Y: Cold Spring Harbor Laboratory Press.

Henríquez, V., Escobar, C., Galarza, J., & Gimpel, J. (2016). Carotenoids in Microalgae. In C. Stange (Ed.), *Carotenoids in Nature: Biosynthesis, Regulation and Function* (pp. 219–237). doi: 10.1007/978-3-319-39126-7_8

Hou, X. (2012). Anaerobic xylose fermentation by *Spathaspora passalidarum*. *Applied Microbiology and Biotechnology*, *94*(1), 205–214. doi: 10.1007/s00253-011-3694-4

Irwandi Jaswir. (2011). Carotenoids: Sources, medicinal properties and their application in food and nutraceutical industry. *Journal of Medicinal Plants Research*, *5*(33). doi: 10.5897/JMPRX11.011

Jin, Yong-Su, Lee, T. H., Choi, Y. D., Ryu, Y. W., & Seo, J. H. (2000). Conversion of xylose to ethanol by recombinant *Saccharomyces cerevisiae* containing genes for xylose reductase and xylitol dehydrogenase from Pichia stipitis. *Journal of Microbiology and Biotechnology*, *10*(4), 564–567.

Jin, Y.-S., Laplaza, J. M., & Jeffries, T. W. (2004). *Saccharomyces cerevisiae* Engineered for Xylose Metabolism Exhibits a Respiratory Response. *Applied and Environmental Microbiology*, *70*(11), 6816–6825. doi: 10.1128/AEM.70.11.6816-6825.2004

Kim, S. R., Ha, S.-J., Wei, N., Oh, E. J., & Jin, Y.-S. (2012). Simultaneous co-fermentation of mixed sugars: A promising strategy for producing cellulosic ethanol. *Trends in Biotechnology*, *30*(5), 274–282. doi: 10.1016/j.tibtech.2012.01.005

Kim, S. R., Skerker, J. M., Kang, W., Lesmana, A., Wei, N., Arkin, A. P., & Jin, Y.-S. (2013). Rational and Evolutionary Engineering Approaches Uncover a Small Set of Genetic Changes Efficient for Rapid Xylose Fermentation in *Saccharomyces cerevisiae*. *PLOS ONE*, *8*(2), e57048. doi: 10.1371/journal.pone.0057048

Kok, S., Nijkamp, J. F., Oud, B., Roque, F. C., Ridder, D., Daran, J.-M., … Maris, A. J. A. (2012). Laboratory evolution of new lactate transporter genes in a jen1Δ mutant of *Saccharomyces cerevisiae* and their identification as *ADY2* alleles by whole-genome resequencing and transcriptome analysis. *FEMS Yeast Research*, *12*(3), 359–374. doi: 10.1111/j.1567-1364.2011.00787.x

Kwak, S., Jo, J. H., Yun, E. J., Jin, Y.-S., & Seo, J.-H. (2019). Production of biofuels and chemicals from xylose using native and engineered yeast strains. *Biotechnology Advances*, *37*(2), 271–283. doi: 10.1016/j.biotechadv.2018.12.003

Kwak, S., Kim, S. R., Xu, H., Zhang, G.-C., Lane, S., Kim, H., & Jin, Y.-S. (2017). Enhanced isoprenoid production from xylose by engineered *Saccharomyces cerevisiae*. *Biotechnology and Bioengineering*, *114*(11), 2581–2591. doi: 10.1002/bit.26369

Li, Q., Sun, Z., Li, J., & Zhang, Y. (2013). Enhancing beta-carotene production in *Saccharomyces cerevisiae* by metabolic engineering. *FEMS Microbiology Letters*, *345*(2), 94–101. doi: 10.1111/1574-6968.12187

555 Livak, K. J., & Schmittgen, T. D. (2001). Analysis of Relative Gene Expression Data Using
556 Real-Time Quantitative PCR and the $2^{-\Delta\Delta CT}$ Method. *Methods*, *25*(4), 402–408. doi:
557 10.1006/meth.2001.1262
558 López, J., Cataldo, V. F., Peña, M., Saa, P. A., Saitua, F., Ibaceta, M., & Agosin, E. (2019).
559 Build Your Bioprocess on a Solid Strain—β-Carotene Production in Recombinant
560 *Saccharomyces cerevisiae*. *Frontiers in Bioengineering and Biotechnology*, *7*. doi:
561 10.3389/fbioe.2019.00171
562 Ma, T., Shi, B., Ye, Z., Li, X., Liu, M., Chen, Y., … Liu, T. (2019). Lipid engineering
563 combined with systematic metabolic engineering of *Saccharomyces cerevisiae* for
564 high-yield production of lycopene. *Metabolic Engineering*, *52*, 134–142. doi:
565 10.1016/j.ymben.2018.11.009
566 Matsushika, A., Goshima, T., & Hoshino, T. (2014). Transcription analysis of recombinant
567 industrial and laboratory *Saccharomyces cerevisiae* strains reveals the molecular basis
568 for fermentation of glucose and xylose. *Microbial Cell Factories*, *13*(1), 16. doi:
569 10.1186/1475-2859-13-16
570 Meadows, A. L., Hawkins, K. M., Tsegaye, Y., Antipov, E., Kim, Y., Raetz, L., … Tsong, A.
571 E. (2016). Rewriting yeast central carbon metabolism for industrial isoprenoid
572 production. *Nature*, *537*(7622), 694–697. doi: 10.1038/nature19769
573 Montanti, J., Nghiem, N. P., & Johnston, D. B. (2011). Production of Astaxanthin from
574 Cellulosic Biomass Sugars by Mutants of the Yeast *Phaffia rhodozyma*. *Applied*
575 *Biochemistry and Biotechnology*, *164*(5), 655–665. doi: 10.1007/s12010-011-9165-7
576 Palozza, P., & Krinsky, N. I. (1992). [38] Antioxidant effects of carotenoids in Vivo and in
577 Vitro: An overview. In *Carotenoids Part A: Chemistry, Separation, Quantitation, and*
578 *Antioxidation*: *Vol. 213*. *Methods in Enzymology* (pp. 403–420). doi: 10.1016/0076-
579 6879(92)13142-K

Peralta-Yahya, P. P., Ouellet, M., Chan, R., Mukhopadhyay, A., Keasling, J. D., & Lee, T. S. (2011). Identification and microbial production of a terpene-based advanced biofuel. *Nature Communications*, *2*(1), 483. doi: 10.1038/ncomms1494

Pfeiffer, T., & Morley, A. (2014). An evolutionary perspective on the Crabtree effect. *Frontiers in Molecular Biosciences*, *1*. doi: 10.3389/fmolb.2014.00017

Reyes, L. H., Gomez, J. M., & Kao, K. C. (2014). Improving carotenoids production in yeast via adaptive laboratory evolution. *Metabolic Engineering*, *21*, 26–33. doi: 10.1016/j.ymben.2013.11.002

Ro, D.-K., Paradise, E. M., Ouellet, M., Fisher, K. J., Newman, K. L., Ndungu, J. M., … Keasling, J. D. (2006). Production of the antimalarial drug precursor artemisinic acid in engineered yeast. *Nature*, *440*(7086), 940. doi: 10.1038/nature04640

Sorger, D., Athenstaedt, K., Hrastnik, C., & Daum, G. (2004). A Yeast Strain Lacking Lipid Particles Bears a Defect in Ergosterol Formation. *Journal of Biological Chemistry*, *279*(30), 31190–31196. doi: 10.1074/jbc.M403251200

Sun, L., Kwak, S., & Jin, Y.-S. (2019). Vitamin A Production by Engineered *Saccharomyces cerevisiae* from Xylose via Two-Phase in Situ Extraction. *ACS Synthetic Biology*, *8*(9), 2131–2140. doi: 10.1021/acssynbio.9b00217

Sun, Y., Sun, L., Shang, F., & Yan, G. (2016). Enhanced production of β-carotene in recombinant *Saccharomyces cerevisiae* by inverse metabolic engineering with supplementation of unsaturated fatty acids. *Process Biochemistry*, *51*(5), 568–577. doi: 10.1016/j.procbio.2016.02.004

van Hoek, P., de Hulster, E., van Dijken, J. P., & Pronk, J. T. (2000). Fermentative capacity in high-cell-density fed-batch cultures of baker's yeast. *Biotechnology and Bioengineering*, *68*(5), 7.

Verwaal, R., Wang, J., Meijnen, J.-P., Visser, H., Sandmann, G., Berg, J. A. van den, & Ooyen, A. J. J. van. (2007). High-Level Production of Beta-Carotene in *Saccharomyces cerevisiae* by Successive Transformation with Carotenogenic Genes from *Xanthophyllomyces dendrorhous*. *Appl. Environ. Microbiol.*, *73*(13), 4342–4350. doi: 10.1128/AEM.02759-06

Vickers, C. E., Williams, T. C., Peng, B., & Cherry, J. (2017). Recent advances in synthetic biology for engineering isoprenoid production in yeast. *Current Opinion in Chemical Biology*, *40*, 47–56. doi: 10.1016/j.cbpa.2017.05.017

Williams, A. W., Boileau, T. W.-M., Zhou, J. R., Clinton, S. K., & Erdman, J. W. (2000). β-Carotene Modulates Human Prostate Cancer Cell Growth and May Undergo Intracellular Metabolism to Retinol. *The Journal of Nutrition*, *130*(4), 728–732. doi: 10.1093/jn/130.4.728

Xie, W., Liu, M., Lv, X., Lu, W., Gu, J., & Yu, H. (2014). Construction of a controllable β-carotene biosynthetic pathway by decentralized assembly strategy in *Saccharomyces cerevisiae*. *Biotechnology and Bioengineering*, *111*(1), 125–133. doi: 10.1002/bit.25002

Xie, W., Lv, X., Ye, L., Zhou, P., & Yu, H. (2015). Construction of lycopene-overproducing *Saccharomyces cerevisiae* by combining directed evolution and metabolic engineering. *Metabolic Engineering*, *30*, 69–78. doi: 10.1016/j.ymben.2015.04.009

Yan, G., Wen, K., & Duan, C. (2012). Enhancement of β-Carotene Production by Over-Expression of HMG-CoA Reductase Coupled with Addition of Ergosterol Biosynthesis Inhibitors in Recombinant *Saccharomyces cerevisiae*. *Current Microbiology*, *64*(2), 159–163. doi: 10.1007/s00284-011-0044-9

Yeum, K. J., Booth, S. L., Sadowski, J. A., Liu, C., Tang, G., Krinsky, N. I., & Russell, R. M. (1996). Human plasma carotenoid response to the ingestion of controlled diets high in

fruits and vegetables. *The American Journal of Clinical Nutrition*, *64*(4), 594–602. doi: 10.1093/ajcn/64.4.594

Yoon, S.-H., Park, H.-M., Kim, J.-E., Lee, S.-H., Choi, M.-S., Kim, J.-Y., … Kim, S.-W. (2007). Increased β-Carotene Production in Recombinant *Escherichia coli* Harboring an Engineered Isoprenoid Precursor Pathway with Mevalonate Addition. *Biotechnology Progress*, *23*(3), 599–605. doi: 10.1021/bp070012p

Yuan, L. Z., Rouvière, P. E., LaRossa, R. A., & Suh, W. (2006). Chromosomal promoter replacement of the isoprenoid pathway for enhancing carotenoid production in *E. coli*. *Metabolic Engineering*, *8*(1), 79–90. doi: 10.1016/j.ymben.2005.08.005

Zhang, S., Skerker, J. M., Rutter, C. D., Maurer, M. J., Arkin, A. P., & Rao, C. V. (2016). Engineering *Rhodosporidium toruloides* for increased lipid production. *Biotechnology and Bioengineering*, *113*(5), 1056–1066. doi: 10.1002/bit.25864

Zhao, J., Li, Q., Sun, T., Zhu, X., Xu, H., Tang, J., … Ma, Y. (2013). Engineering central metabolic modules of *Escherichia coli* for improving β-carotene production. *Metabolic Engineering*, *17*, 42–50. doi: 10.1016/j.ymben.2013.02.002

Zhou, P., Xie, W., Li, A., Wang, F., Yao, Z., Bian, Q., … Ye, L. (2017). Alleviation of metabolic bottleneck by combinatorial engineering enhanced astaxanthin synthesis in *Saccharomyces cerevisiae*. *Enzyme and Microbial Technology*, *100*, 28–36. doi: 10.1016/j.enzmictec.2017.02.006

Figure captions

Fig. 1. Biosynthetic pathway of β-carotene (**A**) and transcriptional levels of related genes (**C**) on glucose and xylose in engineered *S. cerevisiae*. A heterogolous xylose assimilation pathway containing xylose reductase (XR), xylitol dehydrogenase (XDH) and xylulokinase (XK) is connected with lower glycolytic pathway by pentose phosphate pathway (PPP). Pyruvate is produced from glucose and xylose and converted into cytosolic acetyl-CoA. Yeast synthesizes farnesyl pyrophosphate from cytosolic acetyl-CoA through the mevalonate pathway (MVA), as the common precursor for the biosynthesis of ergosterol and heterogolous β-carotene. HMG-CoA reductase (HMGR) is a key rate limiting enzyme in MVA. Cytosolic acetyl-CoA is also the precursor for yeast lipids synthesis. G6P, glucose-6-phosphate; F6P, fructose-6-phosphate; GAP, glyceraldegyde-3-phosphate; X5P, xyllulose-5-phosphate; IPP, isopentenyl pyrophosphate; DMAPP, dimethylallyl pyrophosphate; GPP, geranyl pyrophosphate; FPP, farnesyl pyrophosphate; GGPP, geranylgeranyl pyrophosphate. Pictures of glucose and xylose cultures of SR8B strain were taken at 30 hour (**B**). Samples for transcriptional analysis were taken at exponetial phase from each condition for RNA extraction and expression level analysis. Fold changes were calculated by dividing genes expression levels on xylose by those on glucose. Three biological replicates and three technical replicates were performed for each gene, and the error bars represented standard deviations.

Fig. 2. The overlaid HPLC chromatograms of carotenoids extracted from the engineered *S. cerevisiae* SR8B cultured on glucose and xylose condition. Cells were cultured in a defined medium containing either 40 g/L glucose or 40 g/L xylose from initial OD_{600} 1. Same amount of cells were harvested at 90 hour from each condition to extract the carotenoids for HPLC chromotography.

Fig. 3. Batch fermentation profiles of the engineered *S. cerevisiae* SR8B on glucose (**A**) and xylose (**B**) conditions and the corresponding β-carotene production patterns on glucose (**C**) and xylose (**D**). Data are presented as mean values and standard deviations of three independent biological replicates.

Fig. 4. Comparison of β-carotene production by the engineered SR8B and SR8BH strains through glucose and xylose utilization. Cells were harvested at the end of fermentation for β-carotene extraction and quantification. Data are presented as mean values and standard deviations of three independent biological replicates

Fig. 5. Ergosterol production (**A**) and lipid bodies visualization (**B**) of the engineered SR8B strain on glucose and xylose . Cells were harvested at the end of fermentation for ergosterol extractiona and quantification. Cells for lipid bodies visualization were harvested at exponential phase and stained with Nile Red fluorescent dye. The stained cells were then viewd under a confocal microscope with 63× oil immersion objective at 633 nm.

Fig. 6 Xylose feb-batch fermentation of the SR8B strain in a 3-litter bioreactor. The bioreactor picture on the right was taken at 80 h.

695 Fig. 1

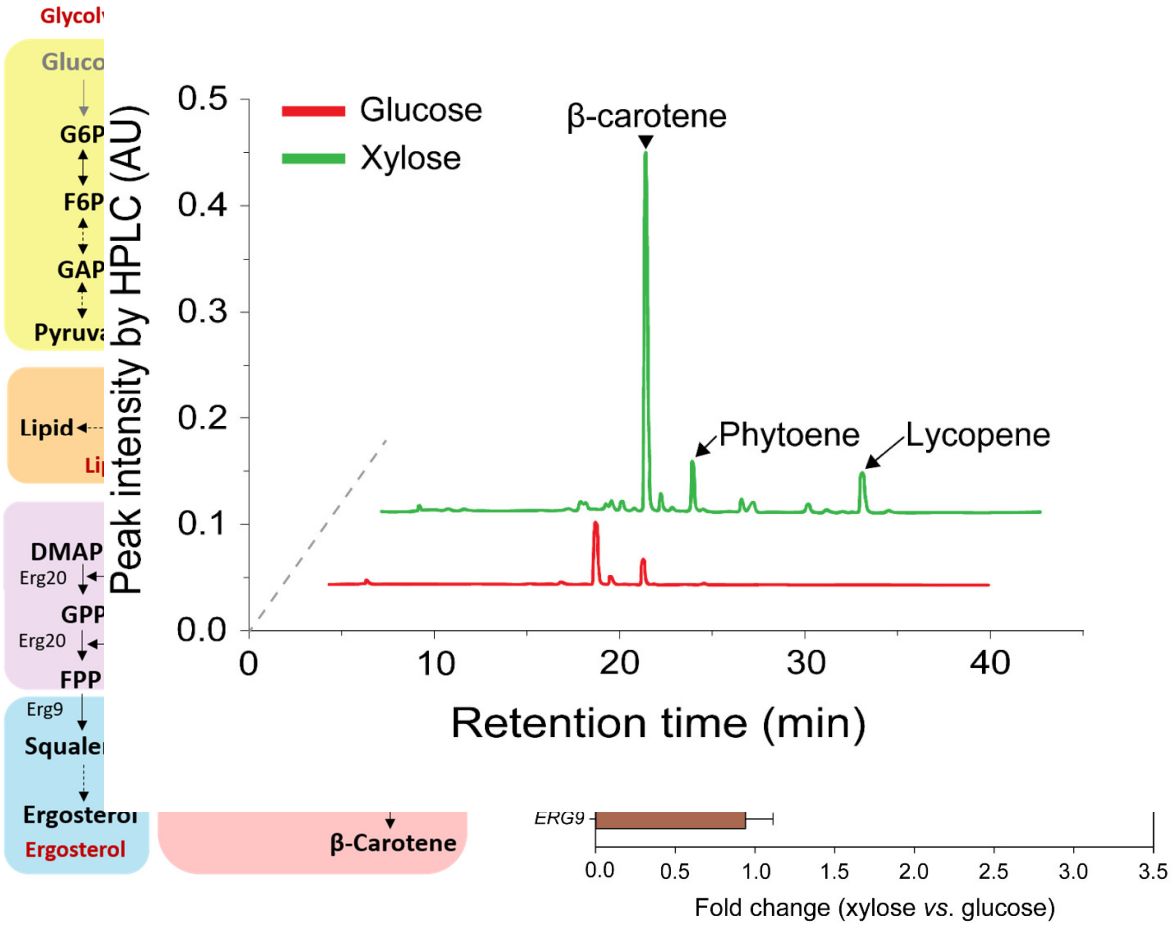

696
697 **Fig. 1A.** Biosynthetic pathway of β-carotene (**A**) and transcriptional levels of related genes (**C**) on
698 glucose and xylose in engineered *S. cerevisiae*. A heterogolous xylose assimilation pathway
699 containing xylose reductase (XR), xylitol dehydrogenase (XDH) and xylulokinase (XK) is connected
700 with lower glycolytic pathway by pentose phosphate pathway (PPP). Pyruvate is produced from
701 glucose and xylose and converted into cytosolic acetyl-CoA. Yeast synthesizes farnesyl
702 pyrophosphate from cytosolic acetyl-CoA through the mevalonate pathway (MVA), as the common
703 precursor for the biosynthesis of ergosterol and heterogolous β-carotene. HMG-CoA reductase
704 (HMGR) is a key rate limiting enzyme in MVA. Cytosolic acetyl-CoA is also the precursor for yeast
705 lipids synthesis. G6P, glucose-6-phosphate; F6P, fructose-6-phosphate; GAP, glyceraldegyde-3-
706 phosphate; X5P, xyllulose-5-phosphate; IPP, isopentenyl pyrophosphate; DMAPP, dimethylallyl
707 pyrophosphate; GPP, geranyl pyrophosphate; FPP, farnesyl pyrophosphate; GGPP, geranylgeranyl
708 pyrophosphate. Pictures of glucose and xylose cultures of SR8B strain were taken at 30 hour (**B**).
709 Samples for transcriptional analysis were taken at exponetial phase from each condition for RNA
710 extraction and expression level analysis. Fold changes were calculated by dividing genes expression
711 levels on xylose by those on glucose. Three biological replicates and three technical replicates were
712 performed for each gene, and the error bars represented standard deviations.
713 Fig. 2
714

Fig. 2. The overlaid HPLC chromatograms of carotenoids extracted from engineered *S. cerevisiae* SR8B cultured on glucose and xylose condition. Cells were cultured in defined medium containing either 40 g/L glucose or 40 g/L xylose from initial OD_{600} 1. Same amount of cells were harvested at 90

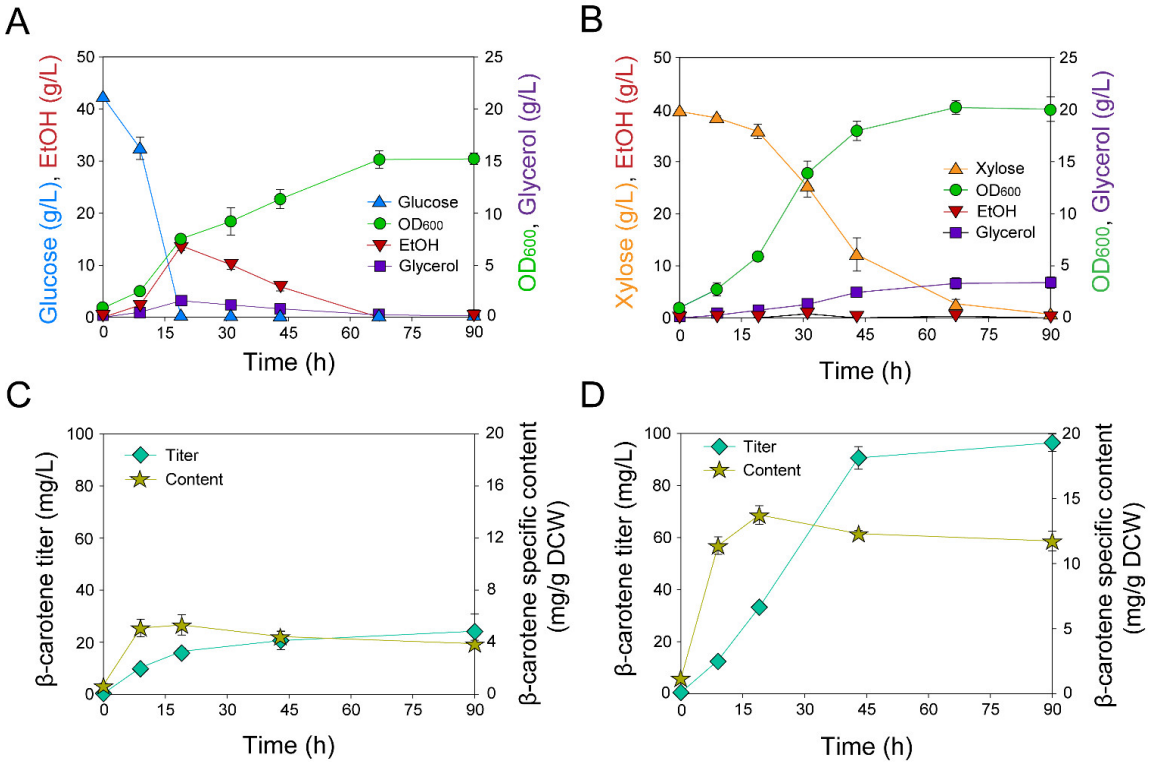

hour from each condition to extract the carotenoids for HPLC chromotography.

Fig. 3

Fig. 3. Batch fermentation profiles of engineered *S. cerevisiae* SR8B on glucose (**A**) and xylose (**B**) conditions and the corresponding β-carotene production patterns on glucose (**C**) and xylose (**D**). Data are presented as mean values and standard deviations of three independent biological replicates.

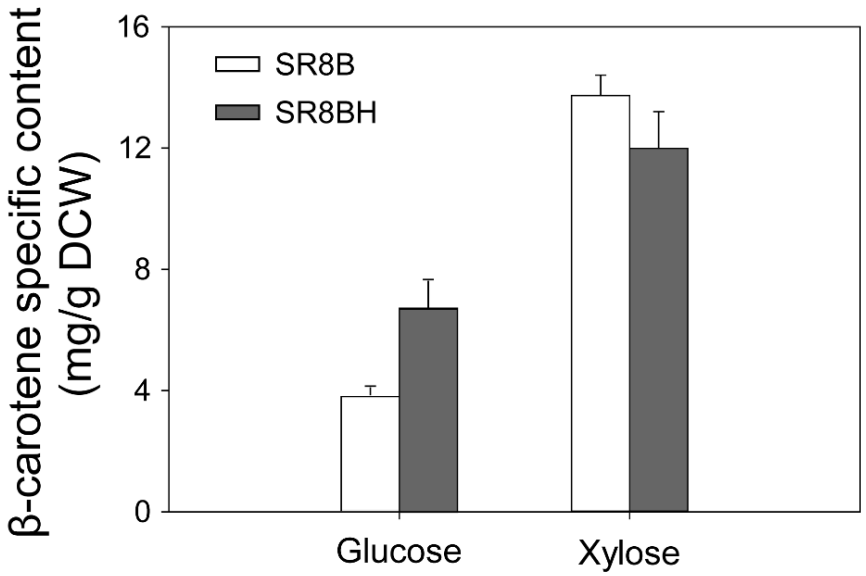

726 Fig. 4

727

728 **Fig. 4**. Comparison of β-carotene production by engineered SR8B and SR8BH strains through glucose
729 and xylose utilization. Cells were harvested at the end of fermentation for β-carotene extraction and
730 quantification. Data are presented as mean values and standard deviaitons of three independent
731 biological replicates
732

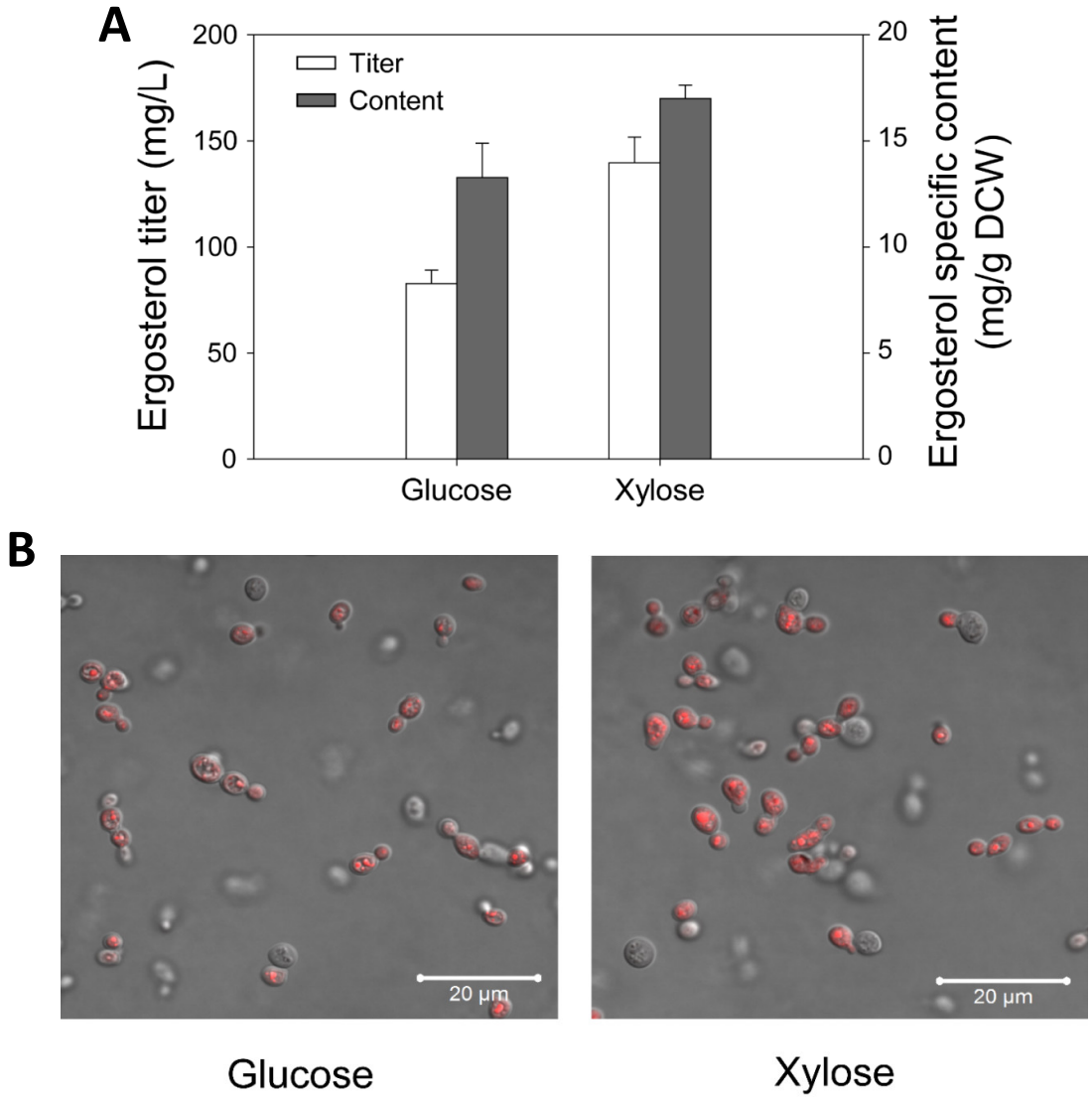

733 Fig. 5

734

735 **Fig. 5**. Ergosterol production (**A**) and lipid bodies visualization (**B**) of the engineered SR8B strain on
736 glucose and xylose . Cells were harvested at the end of fermentation for ergosterol extractiona and
737 quantification. Cells for lipid bodies visualization were harvested at exponential phase and stained
738 with Nile Red fluorescent dye. The stained cells were then viewd under a confocal microscope with
739 63× oil immersion objective at 633 nm.
740

741 Fig. 6

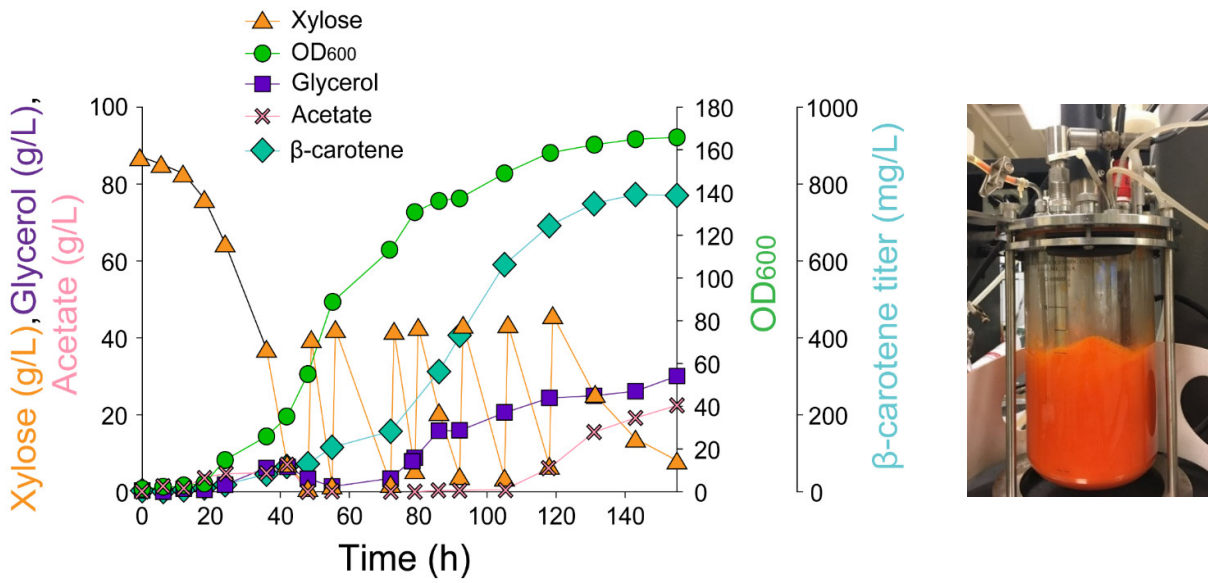

742

743 **Fig. 6** Xylose feb-batch fermentation of the SR8B strain using Verduyn medium. The bioreactor
744 picture on the right was taken at 80 h.
745

746 **Table 1. Strains and plasmids used in this study.**

Name	Description	Source
Strains		
E.coli DH5α	*F-, ϕ80d, lacZΔM15, endA1, recA1, hsdR17 (rK-mK), supE44, thi-1, gyrA96, relA1*	Invitrogen, CA
S. cerevisiae SR8	D452-2 expressing *XYL1*, *XYL2*, and *XKS1* through integration, evolutionary engineering in xylose-containing media, and *ALD6* deletion	(Kim et al., 2013)
S. cerevisiae SR8U-	SR8 with *URA3* disrupted as an auxotrophic marker	This study
S. cerevisiae SR8B	SR8U- ura3: *URA3* YIplac211YB/I/E*	This study
S. cerevisiae SR8BH	SR8B with integrated pTDH3-tHMG1-tCYC1 in the CS5 locus	This study
Plasmids		
YIplac211YB/I/E*	YIplac211 *TDH3p-crtYB-CYC1t*; *TDH3p-crtI-CYC1t*; *TDH3p-crtE*-CYC1t*	(Verwaal et al., 2007)
Cas9-NAT	Cas9 expression plasmid, NAT1 marker	(Zhang et al., 2014)

gRNA-ura-HYB	*URA3* disruption gRNA cassette, HyB marker	(Zhang et al., 2014)
pRS425TDH-tHMG1	pRS425 plasmid with pTDH3-tHMG1-tCYC1 cassette	(Kwak et al., 2017)
pRS42H-CS5	pRS42H with gRNA cassette targeting the intergenic site CS5	(Kwak et al., 2017)

747